Bistability and chaos in an injection-locked semiconductor laser

Eok-Kyun Lee and Hyun-Soo Pang
Department of Chemistry, Korea Advanced Institute of Science and Technology, Taejon 305–701, Republic of Korea
Jong-Dae Park
Department of Physics, Pai-Chai University, Taejon 302–162, Republic of Korea
Hoyun Lee
Department of Physics, Chungnam National University, Taejon 305–764, Republic of Korea
(Received 25 February 1992; revised manuscript received 7 August 1992)

We present a theoretical investigation of complex dynamical behaviors of an injection-locked semiconductor laser. A period-doubling bifurcation route to chaos and bistability has been identified. The boundaries for period-doubling bifurcations and chaos are mapped out in the injection-level–frequency-detuning plane. It was shown that there exist two locally stable attractors of limit cycles. The centers of the attractors shift nonlinearly with injection level. The shift of the center of the electric-field phase is estimated by the harmonic balance method.

PACS number(s): 42.50.Lc, 05.45.+b, 42.55.Px

I. INTRODUCTION

The nonlinear dynamical properties of optical systems are currently of great theoretical and practical interest. Especially, the nonlinear phenomena observed in semiconductor lasers deserve special attention due to their effects in the applications such as optical communications, optical fiber sensors, and high-resolution spectroscopy. They are also interesting theoretical subjects due to their possibilities of showing bifurcations and deterministic chaos [1–10]. The complex dynamical phenomena in semiconductor lasers have often been induced by the coherent optical feedback [1–4], direct current modulation [5], or by the injection of coherent light [6–10].

Studies on the nonlinear dynamical behavior of injection-locked semiconductor lasers have been initiated by a pioneering work of Lang [6]. Otsuka and Kawaguchi [7] predicted a period-doubling route to chaos in a detuned-laser system with injected signals. A semiconductor laser may be considered as a detuned laser and their results are also true for the injection-locked semiconductor lasers. Recently, Sacher *et al.* [8] confirmed the route to chaos by numerical simulations. They demonstrated the importance of the linewidth enhancement factor and nonlinear gain for the nonlinear dynamical behaviors. Similar behaviors have been studied in delayed-feedback geometries [2,9,10]. Tromborg and Mørk [2] have employed an injection-locking model to explain the onset of the coherence collapse in external-cavity semiconductor lasers and demonstrated that a period-doubling route to chaos exists for a mode with minimum carrier density. They also observed quasiperiodic behavior and frequency locking for a mode with minimum linewidth [3,4]. The strong coupling between the variables has defied analytical approaches and most of theoretical studies have heavily relied upon numerical simulations.

In this paper we have analyzed in detail the nonlinear dynamical behaviors in injection-locked semiconductor lasers and identified the boundaries for a period-doubling bifurcation route to chaos in the frequency-detuning–injection-level plane. We also observed a bistability which is associated with two locally stable attractors at low injection levels. These attractors are generated by the nonzero-amplitude oscillations which tend to shift the center of attractors. The shift of the center of attractors is obtained approximately by the harmonic balance method. Close agreements between analytic results and numerical simulations have been achieved. We observe a quasiperiodic region at the positive frequency detuning. The regions of bistability and quasiperiodicity and the boundaries for linear stability have been mapped out in the frequency-detuning–injection-level plane.

II. THEORY

The conventional rate equations have often been successful to explain the nonlinear dynamical behavior of injection-locked semicondcutor lasers. We assume that the complex field of the slave laser is represented by [11,12]

$$E_{\rm SL}(t) = E_0(t)e^{i[\Omega t+\phi_0(t)]}, \tag{1}$$

and that of the master laser by

$$E_{\rm ML}(t) = E_1 e^{i[\omega t+\phi_1]}, \tag{2}$$

where $E_0(t), E_1, \phi_0(t)$, and ϕ_1 are real valued and Ω is the angular oscillation frequency of the slave laser without the injected signal. $E_0(t)$ is normalized such that $|E_0(t)|^2$ is the photon density and E_1 is regarded as a constant. ϕ_1 can be set to zero without loss of generality. If stable injection locking occurs, the angular frequency $(\Omega+\dot{\phi}_0)$ of the slave laser approaches that of the master laser as time goes on and the phase $\phi_0(t)$ may be expressed as $(\omega-\Omega)t+\phi_L$, where ϕ_L is the constant locked phase. However, if injection locking occurs incompletely due to dynamic instability, the angular frequency of the slave laser may vary around the oscillation frequency of the master laser and the phase $\phi_0(t)$ may be expressed as $(\omega-\Omega)t+\phi_L+\phi(t)$, where $\phi(t)$ accounts for the complex variation of the phase. The characteristic frequency of dynamic instability may be related with either beating between ω and Ω or the relaxation oscillations. The beating between the two frequency components when the frequency of the master laser is outside the frequency-locking range is of little concern in this paper. Instead we are concerned with the nonlinear dynamics related with the undamped relaxation oscillations, which may persist even though the frequency of the master laser is within the locking range. To investigate the dynamical behavior of an injection-locked semiconductor laser, we have used the following differential rate equations [11,12] for the electric-field amplitude $E_0(t)$ and phase $\phi(t)$ of the slave laser:

$$\frac{dE_0}{dt} = \tfrac{1}{2}G_N(N - N_{\rm th})E_0(t) + \frac{1}{\tau_{\rm in}}E_1 \cos[\phi_L + \phi(t)], \tag{3}$$

$$\frac{d\phi}{dt} = -(\omega - \Omega) + \tfrac{1}{2}\alpha G_N(N - N_{\rm th}) - \frac{1}{\tau_{\rm in}}\frac{E_1}{E_0(t)}\sin[\phi_L + \phi(t)]. \tag{4}$$

The coupling between the real and imaginary part of the refractive index is represented by the linewidth enhancement factor α. The gain G per unit time is assumed to be given by $G(N) = G_N(N - N_0)$, where N is the carrier density in the active region, $G_N = \partial G/\partial N$ is the differential gain, and N_0 is the carrier density required for transparency. The threshold carrier density $N_{\rm th}$ for the slave laser is related to the photon lifetime τ_p by the threshold condition that the gain equals the loss [i.e., $G(N_{\rm th}) = 1/\tau_p$]. $\tau_{\rm in}$ is the diode cavity round-trip time.

The temporal evolution of the carrier density is governed by the usual rate equation

$$\frac{dN}{dt} = J - \frac{N(t)}{\tau_s} - G(N)|E_0(t)|^2, \tag{5}$$

where J is the carrier injection rate per unit volume and τ_s is the spontaneous carrier lifetime.

The stationary solutions of these rate equations can be found to be [10]

$$E_{0,\rm st}^2 = \tau_p\left(J - \frac{N_{\rm st}}{\tau_s}\right), \tag{6}$$

$$N_{\rm st} = N_{\rm th} - 2\frac{1}{\tau_{\rm in}G_N}\frac{E_1}{E_{0,\rm st}}\cos\phi_L, \tag{7}$$

$$\Delta\omega = \omega - \Omega = -\frac{1}{\tau_{\rm in}}\frac{E_1}{E_{0,\rm st}}[\sin\phi_L + \alpha\cos\phi_L]. \tag{8}$$

The stable frequency-locking range can be found from the following considerations: (a) the range of allowed frequency detuning and (b) dynamical stability. The condition (a) leads to the following frequency-detuning range:

$$-\Delta\omega_L \le \Delta\omega \le \Delta\omega_L,\ \Delta\omega_L = \frac{1}{\tau_{\rm in}}\frac{E_1}{E_{0,\rm st}}(1+\alpha^2)^{\frac{1}{2}}. \tag{9}$$

The condition (b) for dynamical stability of the injection-locked semiconductor lasers further limits the frequency-locking range. For a given $\Delta\omega$, the stable locked-phase ϕ_L is

$$\phi_L = -\sin^{-1}\left(\frac{\Delta\omega}{\Delta\omega_L}\right) - \tan^{-1}\alpha. \tag{10}$$

However, the linear stability analysis can provide only the condition for the Hopf bifurcation which is due to the undamping of the relaxation oscillations.

When the amplitudes of oscillations are small, periodic nonlinear behaviors can be studied by the harmonic balance method. Once the oscillations occur, the steady-state values $E_{0,\rm st}$, ϕ_L, and $N_{\rm st}$ no longer serve to be the centers of oscillations. Consequently, the shift of the center of oscillations should be considered. Oscillations of electric-field amplitude and carrier density can be approximated to be

$$E_0(t) = \tilde{E}_0 + \epsilon_a \sin(\Omega_R t + \psi_E), \tag{11}$$

$$N(t) = \tilde{N} + n_a \sin(\Omega_R t + \psi_N), \tag{12}$$

where $\tilde{E}_0$ and $\tilde{N}$ are the time average value of electric-field amplitude and carrier density, respectively. ϵ_a and n_a are the oscillation amplitudes of $E_0(t)$ and $N(t)$. ψ_E accounts for the phase delay of $E(t)$ with respect to $\phi(t)$, while ψ_N accounts for the phase delay of $N(t)$. Ω_R is the angular oscillation frequency. The numerical simulations show that the shift ϕ_s is large compared to the shift of centers of $E(t)$ and $N(t)$. Thus $\phi(t)$ is approximated to be

$$\phi(t) = \phi_s + \phi_a \sin(\Omega_R t), \tag{13}$$

where ϕ_s accounts for the shift of the center of $\phi(t)$ from the steady-state locked phase ϕ_L and ϕ_a is the amplitude of oscillations of $\phi(t)$. By taking the time average of the rate equation (3)–(5), ϕ_s can be calculated as a function of the injection level. The study of nonlinear dynamics in the region where the harmonic balance method fails may be conducted via numerical simulation of the rate equations.

III. RESULTS AND DISCUSSION

The numerical integration of the rate equations was performed using an Adams method with a time step of 10 ps. The laser parameters used in the calculations had the following values: $G_N = 0.6 \times 10^{-12}$ m^3 s^{-1}, $N_0 = 1.2 \times 10^{24}$ m^{-3}, $\tau_s = 2.2$ ns, $\tau_p = 1.5$ ps, $\tau_{\rm in} = 8$ ps, $\alpha = 3$. The injection current $I_{\rm th}$ was 1.03 times the threshold current of the slave laser. The variables are set initially to their steady-state values which are determined by the locked phase, and integration is allowed to proceed for approximately 200 ns before any data are accumulated. This allows any initial transients to die out. The electric-field amplitude, the phase, and the carrier density are computed over 100 ns.

Previously, period-doubling routes to chaos have been identified by varying the frequency detuning [7] or injection level [8]. We have confirmed the period-doubling route to chaos with increasing the injection levels or frequency detuning. Figure 1 shows one of the bifurcation diagrams obtained by sampling only the extrema of the electric-field phase $\phi(t)$ with increasing the injection level. The initial locked phase was chosen to be ϕ_L at the frequency detuning $\Delta f = -20$ MHz. Orbits of period up to $32T$ ($T = 2\pi/\omega_R$) have been identified from the numerical study of the rate equations. The universal constant δ of period-doubling bifurcation has been calculated to be 4.50 from the first three bifurcation injection levels. The chaotic bands of period $4T$ and $2T$

can also be seen in Fig. 1. The chaotic band of period $2T$ becomes a stable orbit of period $4T$ at the injection level $E_1/E_{0,\mathrm{st}} \sim 0.007$. The stable orbit is thought to be related with a periodic window embedded within the chaotic regime. The period-doubling route to chaos has also been observed at different frequency-detuning values. The mechanism of period-doubling bifurcation is thought to be due to the coupling introduced by the linewidth enhancement factor in Eq. (4). The strong modulation induced by the light injection also seems to play an important role in the period-doubling route to chaos. A period-doubling route to chaos has been previously observed in direct modulated semiconductor lasers [5]. The period-doubling bifurcations up to infinite periods and inverse period-doubling bifurcations of chaotic bands are well-known behavior in the logistic map or forced limit cycle oscillators (for example, the Brusselator) [13]. Figure 2 shows the stable frequency-locking range and critical injection levels for Hopf bifurcation and period-doubling bifurcations at various frequency detunings. The regions of period 2^nT orbits and chaotic bands are indicated as 2^nP and 2^nI, respectively. The regions of chaotic bands are also shown in this figure with their periods. The upper limit of frequency detuning Δf for the period-doubling bifurcations was ranged from 40 to 90 MHz, depending on the injection level. We have also observed very complex behaviors such as periodic motion with a period of $2\times 3T$, $2\times 5T$, $3\times 5T$, etc., at the positive frequency-detuning region and injection level from 0.005 to 0.007, but the boundaries for these orbits were difficult to map out.

Figure 3 shows the change of the oscillation amplitude of the electric field with an increase of positive frequency detuning. Quasiperiodic behavior, which is due to the interaction between the detuning frequency and relaxation oscillation frequency, has been observed at large frequency detuning. The frequency detunings at which period-one oscillations change to quasiperiodic oscillations are shown by the dashed line in Fig. 2. The sudden change of the electric-field oscillation amplitude $E_0(t)$ has occured at a certain frequency detuning as shown in Fig. 3. This critical frequency detuning is marked

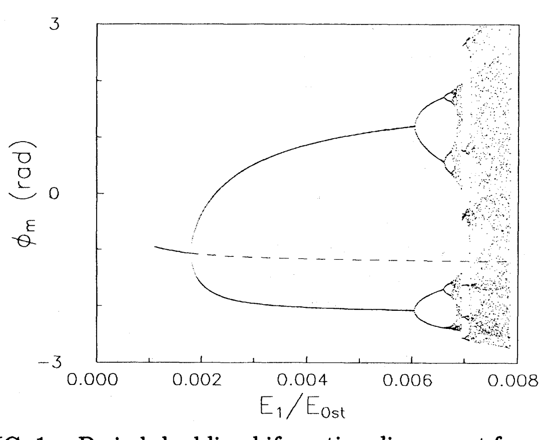

FIG. 1. Period-doubling bifurcation diagram at frequency detuning $\Delta f = -20$ MHz. The extrema of the electric-field phase ϕ_m are sampled. The dashed line indicates ϕ_L.

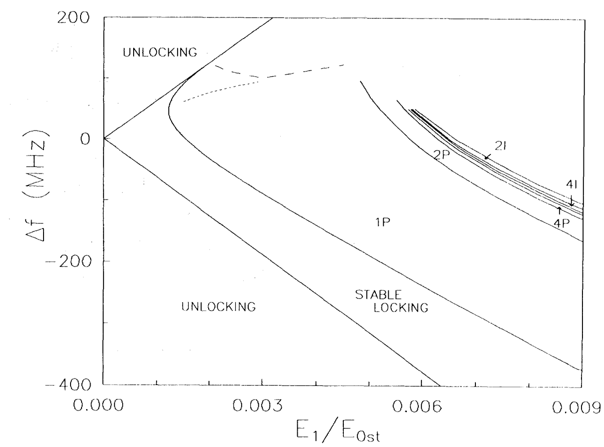

FIG. 2. Boundaries for period-doubling bifurcations and chaos in the frequency-detuning Δf and injection-level $E_1/E_{0,\mathrm{st}}$ plane. The frequency detuning for the transition of an attractor and the detuning for quasiperiodicity are shown by a dotted line and dashed line, respectively.

by a dotted line in Fig. 2. To explain the discontinuous change of the amplitude of oscillations, we have projected the attractors onto the $\phi(t)$ vs $E_0(t)$ plane as shown in Fig. 4. The attractor to which the system eventually approaches is determined by the initial conditions. Figure 4 shows such an initial-value dependent behavior: The upper cycle has been reached when the initial values of the phase and electric-field amplitude are chosen to be those indicated as open circles in Fig. 4, while the lower cycle has been obtained when the initial values are chosen to be those indicated as closed circles. The initial carrier density was set to equal the steady-state value. The projected center of one attractor lies above the value of the steady-state locked phase ϕ_L, while it lies below the steady-state locked phase for the other attractor.

It may be noticed that the center of periodic oscillation moves from the steady-state solutions of the rate equations. The nonlinear shift of the center of periodic

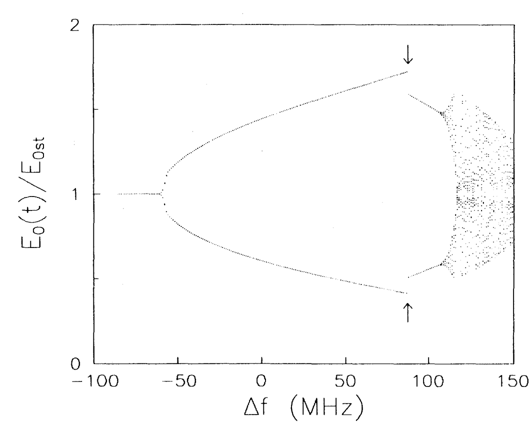

FIG. 3. The magnitude of the relative electric-field amplitude $E_0(t)/E_{0,\mathrm{st}}$ with frequency detuning at the injection level $E_1/E_{0,\mathrm{st}} = 0.0025$. The limit cycle formed by an attractor transits to the other one governed by another attractor at the frequency detuning $\Delta f = 87$ MHz.

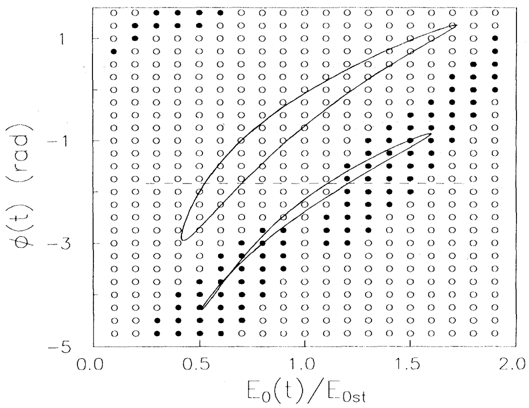

FIG. 4. Projection of attractors onto the $E_0(t)$ vs $\phi(t)$ plane. Injection level $E_1/E_{0,\mathrm{st}} = 0.0025$, frequency detuning $\Delta f = 87$ MHz. The dashed line indicates ϕ_L obtained from Eq. (10). The upper orbit can be reached from the initial points marked with open circles, whereas the lower one can be reached from the initial points marked with closed circles.

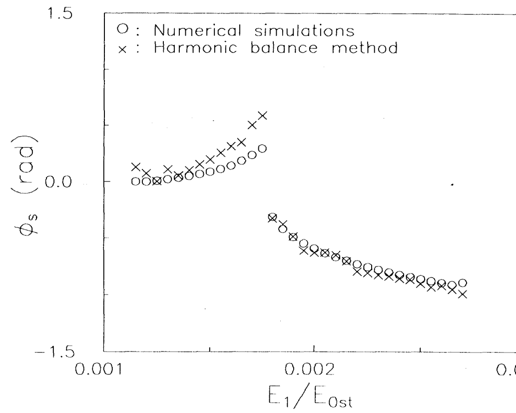

FIG. 5. Shifts of the center of an attractor as a function of the injection level along the line $\Delta\omega = 2.06\frac{1}{\tau_{\mathrm{in}}}\frac{E_1}{E_{0,\mathrm{st}}}$. The symbol ∘ denotes the results obtained from numerical simulations, while × denotes those from the harmonic balance method.

orbit is believed to generate a bistability. The bistability, which is generated between the stable orbits, is different from the common bistabilities associated with two stable fixed points. We have examined the shifts of the center using the harmonic balance method. The oscillation amplitudes as a function of injection levels are obtained from numerical simulations. ψ_E and ψ_N are approximately determined from a linear stability analysis. Then the shifts of the centers are calculated. The centers of the electric-field amplitude and carrier density do not shift significantly from their steady-state values. But the center of the electric-field phase is shown to shift significantly. Figure 5 shows shifts of the center of $\phi(t)$ as a function of the injection level. The frequency detuning $\Delta\omega$ was varied with the injection level such that $\Delta\omega = 2.06\frac{1}{\tau_{\mathrm{in}}}\frac{E_1}{E_{0,\mathrm{st}}}$. Close agreements between the results of numerical simulations and the harmonic balance method have been observed for the frequency detuning above the critical frequency detuning, while poor agreements have been achieved for the frequency detuning lower than the critical frequency detuning.

IV. CONCLUSIONS

The nonlinear dynamical behaviors of injection-locked semiconductor lasers have been investigated from numerical solutions of the rate equations. The period-doubling route to chaos is confirmed with the variation of the injection level and frequency detuning. Orbits of period up to $32T$, periodic windows, chaotic bands, and bistability have been identified. The boundaries for period-doubling bifurcation and the chaotic regimes are mapped out in the injection-level versus frequency-detuning plane. The shifts of the centers of attractors have been predicted by the harmonic balance method and compared with those obtained by numerical simulations. The existence of two attractors (limit cycles) at a low injection level and positive frequency-detuning regime has been demonstrated.

ACKNOWLEDGMENTS

This work is supported by Korea Advanced Institute of Science and Technology (Eok-Kyun Lee) and Non-directed Research Fund, Korea Research Foundation (Hoyun Lee).

[1] T. Mukai and K. Otsuka, Phys. Rev. Lett. **55**, 1711 (1985).
[2] B. Tromborg and J. Mørk, IEEE J. Quantum Electron. **QE-26**, 642 (1990).
[3] B. Tromborg and J. Mørk, IEEE Photonics Technol. Lett. **2**, 549 (1990).
[4] J. Mørk, J. Mark, and B. Tromborg, Phys. Rev. Lett. **65**, 1999 (1990).
[5] C.-H. Lee, T.-H. Yoon, and S.-Y. Shin, Appl. Phys. Lett. **46**, 95 (1985).
[6] R. Lang, IEEE J. Quantum Electron. **QE-18**, 976 (1982).
[7] K. Otsuka and H. Kawaguchi, Phys. Rev. A **29**, 2953 (1984).
[8] J. Sacher, D. Baums, P. Panknin, W. Elsässer, and E. O. Göbel, Phys. Rev. A **45**, 1893 (1992).
[9] K. Otsuka and H. Iwamura, Phys. Rev. A **28**, 3153 (1983).
[10] K. Otsuka, J. Opt. Soc. Am. B **2**, 168 (1985).
[11] F. Mogensen, H. Olesen, G. Jacobson, IEEE J. Quantum Electron. **QE-21**, 784 (1985).
[12] I. Petitbon, P. Gallion, G. Debarge, and C. Chabran, IEEE J. Quantum Electron. **QE-24**, 148 (1988).
[13] B. Hao and S. Zhang, J. Stat. Phys. **28**, 769 (1982).